A fraction of *Prunella vulgaris* spike extract inhibited neutrophil elastase and protected mice against lipopolysaccharide-induced acute lung injury

Huang-Ping Yu
Chang Gung Memorial Hospital
Chieh-Lun Cheng
Chang Gung University
Kowit-Yu Chong
Chang Gung University
Yu-Ling Huang
Chang Gung University
Kung-Ju Chen
Chang Gung University
Yu-Li Chen
Chang Gung University
Pei-Wen Hsieh (pewehs@mail.cgu.edu.tw)
Chang Gung University https://orcid.org/0000-0002-8882-4711

Research

Keywords: Neutrophil elastase, Acute lung injury, Prunella vulgaris, Traditional Chinese medicines, Bioactivity-guided fractionation

Posted Date: May 21st, 2020

DOI: https://doi.org/10.21203/rs.3.rs-29054/v1

Abstract

Background

Human neutrophil elastase (HNE) is an abundantly expressed neutrophil serine protease that promotes neutrophil invasion and neutrophil extracellular trap (NET) formation, thereby mediating lung tissue destruction and enhancing pulmonary inflammation in acute lung injury (ALI). Chemical agents that target HNE and manipulate HNE level homeostasis are desired to prevent or treat ALI.

Methods

In a search for HNE inhibitors, traditional Chinese medicines were evaluated, leading to the identification of the water extract of spikes of *Prunella vulgaris* as an inhibitor of HNE activity. Using bioactivity-guided fractionation, a bioactive fraction (PVAP) that inhibited NHE activity was prepared, and its effects on lipopolysaccharide (LPS)-induced ALI were studied.

Results

The results suggested that PVAP elicited protective effects against LPS-induced ALI by inhibiting HNE activity, thereby reducing neutrophil invasion, pro-inflammatory cytokine release, and NET formation.

Conclusions

These findings illustrated the utility of PVAP as an agent for preventing ALI.

1. Background

Acute lung injury (ALI) and acute respiratory distress syndrome, as common complications of pneumonia, severe sepsis, trauma, and inhalation injury, are cardiopulmonary diseases with high mortality rates [1, 2]. No effective therapeutic agents are available for ALI, and supportive care is the typical clinical approach [1, 3]; thus, new agents to treat or prevent ALI are needed.

Neutrophils play a pivotal role in the pathology of ALI. During acute inflammation, neutrophils serve as the first line of defense in the innate immune system by activating and recruiting circulating neutrophils to sites of inflammation, after which neutrophil serine proteases (NSPs), reactive oxygen species, and neutrophil extracellular traps (NETs) are generated and released to combat infection [4–6]. Among them, NSPs, such as human neutrophil elastase (HNE), cathepsin G (CG), proteinase 3 (PR3), and NSP4, are mainly released from the azurophilic granules of neutrophils after neutrophil activation. Indeed, HNE is a major NSP that damages both microorganisms and host tissues [6]. Furthermore, HNE can promote neutrophil invasion and NET formation, thereby enhancing pulmonary inflammation [6–8]. Therefore, the

development of chemical agents that target HNE and manipulate HNE level homeostasis may be crucial for preventing or treating ALI.

Drug repositioning is a strategy that re-evaluates existing drugs for new indications, and it has the advantages of rapid incubation and reduced costs in drug research and development [9]. Traditional Chinese medicines (TCMs) have a long history of use, and considerable evidence supports their use for treating and preventing diseases [10–12]. Therefore, TCMs are excellent resources for drug repositioning research.

The dried spikes of *Prunella vulgaris* have been used as traditional medicines and food ingredients for > 100 years in East Asian, European, and American countries, and it is also a major component of famous herbal teas (Wong Lo Kat®) [13, 14]. This plant has antiviral, antibacterial, anti-inflammatory, antitumor, and blood pressure-modulating effects [13, 15–18]. Phytochemical studies isolated triterpenoids [18–20], phenolic acids [21, 22], polysaccharides [23, 24], and flavonoids [13] from *P. vulgaris*.

To identify new HNE inhibitors, 75 water extracts of TCMs were prepared in the present study, and their inhibitory effects on HNE activity were evaluated. Of these, the water extract of *P. vulgaris* spikes (PVW) exhibited inhibitory effects against HNE activity. PVW was subsequently fractionated to isolate the bioactive fractions and/or components that inhibit HNE activity. The effects of the active components of *P. vulgaris* on lipopolysaccharide (LPS)-induced ALI in mice were also evaluated.

2. Experimental

2.1 Materials and reagents

Glucose, mannose, galacturonic acid, rhamnose, galactose, xylose, sodium hydroxide, acetic acid, myeloperoxidase (MPO), LPS (L2280, *Escherichia coli* 055:B5), dexamethasone (DEX), heparin, hydrogen peroxide, bovine serum albumin, *o*-dianisidine dihydrochloride, and phosphate-buffered saline (PBS) were obtained from Sigma-Aldrich (St. Louis, MO, USA). Hydrochloric acid (HCl), sodium citrate dihydrate, and HEPES sodium salt were purchased from J.T Baker (PA, USA). Fucose was procured from Acros Organics (NJ, USA). Arabinose was purchased from Tokyo Chemical Industry (Tokyo, Japan). 1-Phenyl-3-methyl-5-pyrazolone (PMP, A11161) was obtained from Alfa Aesar (MA, USA). HNE, an HNE substrate (methoxysuccinyl-Ala-Ala-Pro-Val-*p*NA), human CG, a human CG substrate (suc-Ala-Ala-Pro-Phe-*p*NA), and a human PR3 substrate (Boc-Ala-Ala-Vna-Sbzl) were acquired from Enzo Life Sciences (NY, USA). PR3 (539483) was procured from Merck (NY, USA). Zoletil® 50 was purchased from Virbac (Carros, France). Xylazine was obtained from Bayer (Seoul, Korea). Isoflurane was acquired from AbbVie (IL, USA). A protein assay kit (#500-0006) was procured from Bio-Rad (CA, USA). ELISA kits for inflammatory cytokines were purchased from eBioscience (CA, USA). Quant-iT PicoGreen was obtained from Invitrogen (MA, USA). Dextran T standards were acquired from Pharmacosmos (Holbaek, Denmark). Anti-MPO antibody (ab9535) was procured from Abcam (Cambridge, UK).

2.2 Genomic identification of the spikes of *P. vulgaris*

To confirm the origin of a TCM that was purchased from a Chinese medicine store (Huang-De-An, New Taipei city, Taiwan), the dried spikes of *P. vulgaris* were identified via ITS sequence and *psb*A-*trn*H sequence analyses (see supplementary material). Then, the sequence similarity (99%) was determined and compared with that in the NCBI genome database (accession # JQ669130 and KX347037).

2.3 Preparation of PVAP

Initially, the bioactive crude polysaccharide fraction (10.5 g) of the dried spikes of *P. vulgaris* (400 g) was prepared as descried previously [25, 26]. Specifically, the crude polysaccharide was dissolved in ddH_2O (1:20, w/v) and sequentially filtrated using Vivaspin 20 (MWCO 100 and 300 kDa, GE Healthcare, Little Chalfont, UK), and then three sub-fractions (<100 kDa, 5.2 g; 100–300 kDa, 3.0 g; and >300 kDa, 2.3 g) were obtained. The middle fraction (2.8 g) was re-dissolved in ddH_2O (50 mg/mL) and centrifuged at 8000 × *g* for 10 min, and then the supernatant was adjusted to pH 3.0 using acetic acid (99.8%). The subsequent precipitate (220 mg, PVAP) was obtained via centrifugation at 8000 × *g* for 10 min. HNE activity assays were then used to monitor the effect of each fraction.

2.4 Physicochemical analysis of PVAP

The carbohydrate, uronic acid, lignin, and protein contents of PVAP were modified and determined as described previously [25, 27]. Briefly, a mixture of 5% (w/v) phenol aqueous solution (30 μL) and concentrated sulfuric acid (150 μL) was added to PVAP or standard (glucose) solution (0.5 mg/mL, 50 μL) and then incubated at 90 °C for 20 min. The products (200 μL) were transferred to 96-well microplates, and their absorbance at 492 nm was monitored. To determine the uronic acid content of PVAP, a sodium tetraborate solution (12.5 mM, 600 μL) was mixed with the PVAP solution (0.5 mg/mL, 100 μL) or with standard (galacturonic acid) solutions (7.81–125 μg/mL, 100 μL) and then incubated at 90 °C for 5 min. Each sample was added into a solution of 0.15% *m*-hydroxydiphenyl and 0.5% sodium hydroxide aqueous solution (10 μL). The mixture was reacted for 5 min, and its absorbance at 520 nm was measured. The amounts of protein in PVAP were determined following the protocol of the Bio-Rad assay kit, and bovine serum albumin (BSA) was used as standard. Briefly, the PVAP solution (0.5 mg/mL, 10 μL) was mixed with Coomassie brilliant blue G-250 (200 μL) and incubated for 5 min at room temperature. The mixture was analyzed at 595 nm using the ELISA reader. To determine its lignin content, PVAP (6 mg) was dissolved in 30% acetyl bromide solution (in glacial acetic acid, 1.5 mL) and incubated at 70 °C for 1 h. The sample was mixed with 2 M sodium hydroxide (2.7 mL), 0.5 M hydroxylamine HCl (0.3 mL), and glacial acetic acid (10.5 mL), and then the UV absorbance of the mixture was recorded at 280 nm. Alkali lignin (Sigma-Aldrich) was used the standard.

2.5 Monosaccharide composition of PVAP

PVAP (10 mg) was transferred into a sealed ampule and then hydrolyzed using 2.0 M trifluoroacetic acid (2 mL) at 100 °C for 8 h, after which the excess trifluoroacetic acid was removed by vacuum. The product and monosaccharide standards (galactose, glucose, galacturonic acid, arabinose, mannose, rhamnose, xylose, fucose, and glucosamine hydrochloride) were dissolved in ddH_2O and conjugated to PMP [26]. The PMP-labeled monosaccharides were analyzed using a Thermo SN4000 HPLC system (MA, USA) equipped with a C18 column (Hypersil™ BDS 5 μm, 4.6 mm × 250 mm, Thermo Fisher) and eluted with a mobile phase of 0.1 M KH_2PO_4, pH 7.0 buffer solution : acetonitrile (83:17). The flow rate was 1 mL/min, the wavelength for UV detection was 245 nm, and injection volume was 20 μL.

2.6 Amino acid analysis

To determine the amino acid residues to which the carbohydrate was linked, PVAP was subjected to reductive alkaline degradation followed by amino acid analysis [28]. Initially, PVAP (20 mg) was cleaved using an alkaline solution (0.25 M sodium hydroxide containing 0.5 M sodium borohydride, 4 mL) at 45 °C for 6 h. The residue (21 mg) was hydrolyzed using 4 N sulfonic acid at 115 °C for 24 h. After cooling, the mixture was neutralized with pyridine, and its pH was adjusted to 6.80. Then, 4 μM dithiothreitol solution (2 mL) was added to the solution, which was incubated at 37 °C for 1 h, and then sodium tetrathionate (120 mg) was added followed by incubation at 25 °C. After 5 h, the mixture was dried by vacuum, and 0.02 N HCl buffer solution (pH 2.2) was added, after which the amino acid residues of protein were established using a Hitachi L-8900 high-speed amino acid analyzer.

2.7 In vitro NSPs activities assay

The HNE enzyme and selectivity assays (CG and PR3) were conducted using 96-well plates as described previously [25, 29]. Briefly, sample or vehicle solution (50 μL) was mixed with 25 μL of enzyme solution (HNE, 5 μM; CG, 10 μM; and PR3, 30 μM), after which 25 μL substrate solution (HNE, 100 μM; PR3, 50 mM; and CG, 10 mM) was added, and the mixture was incubated for up to 30 min (for NE and PR3) or 60 min (for CG). Chromogenic absorbance at 405 nm was monitored used a Thermo Labsystems Multiskan Ascent reader (MA, USA).

2.8 Animal

Male ICR mice (30–35 g, 5–9 weeks old) were purchased from BioLASCO (Ilan, Taiwan). All animal research procedures were reviewed and approved by the Institutional Animal Care and Use Committee of Chang Gung University (Taoyuan, Taiwan, IDs CGU105-019 and CGU16-079). All mice were acclimated for at least 1 week. Animals were granted *ad libitum* access to a commercial rodent diet and drinking water in the Association for Assessment and Accreditation of Laboratory Animal Care-accredited animal facility of Chang Gung University. Mice were housed under constant light conditions (12-h/12-h light/dark). The room temperature was kept at approximately 25 °C, and the relative humidity was maintained at approximately 60%.

2.9 The animal model of LPS-induced ALI.

Male mice (6–9 weeks old) were randomly divided into five groups ($n \geq 6$ in each group) as follows: vehicle, LPS (5 mg/kg), PVAP (125 mg/kg) + LPS, PVAP (250 mg/kg) + LPS, and DEX (10 mg/kg) + LPS. The DEX and LPS solutions were prepared with 10% Tween 80 in sterile PBS. PVAP was dissolved in PBS (100 μL) at a dose equivalent to 125 or 250 mg/kg. Initially, mice were administered PBS, PVAP, or DEX through gavage. After 30 min, mice were anesthetized using a mixture solution of Zoletil® 100 and xylazine (Bayer, Germany) through intraperitoneal injection, and then 50 μL of PBS or LPS (*E. coli* O55:B5, 5 mg/kg) was administrated via intratracheal instillation. After 6 h, mice were sacrificed, and the left lobes of lung tissues were obtained for MPO and HNE activities assays, as well as immunohistochemical (IHC) and hematoxylin and eosin (H&E) staining. The right lobes were harvested for bronchoalveolar lavage fluid (BALF) collection and wet/dry (W/D) ratio analysis.

2.10 Measurement of lung wet to dry (W/D) weight ratios:

The right lobes of lung tissues were harvested and weighted immediately (wet weight). Tissues were transferred to the oven and dried at 80 °C for 72 h, and the dried tissue weight was recorded.

2.11 BALF collection and analysis

The BALF samples were collected as described previously [25, 29]. Briefly, the right lung tissues were lavaged with PBS (1.5 mL) and then centrifuged at 1000 rpm for 15 min at 4 °C, and the supernatant was collected and stored at −80 °C. The total protein concentration of BALF was determined using Bradford protein assay dye (Bio-Rad, 500-0006) with BSA as the standard. Cytokines (IL-6 and TNF-α) levels in BALF were measured using ELISA kits following the manufacturer's instructions. Cell pellets from BALF were re-suspended in PBS (100 μL) and used to prepare cytospin slides. The neutrophil pictures and counts were recorded at ×100 magnification using a Zeiss PrimoStar microscope (Carl Zeiss, Gottingen, Germany). The number of neutrophils was counted in five random fields. To quantify NET DNA, the

amount of dsDNA in BALF was measured using a Quant-iT PicoGreen assay kit per the manufacturer's protocols. In brief, BALF supernatant (100 μL) and standard (lambda DNA) were transferred to a 96-well plates, and then dsDNA staining reagent (100 μL) was added. The mixtures were incubated in the dark for 5 min. The fluorescence absorbance of the mixture was recorded at excitation and emission wavelengths of 485 and 535 nm, respectively.

2.12 Measurement of HNE and MPO activities in the lungs

HNE and MPO activities in lung homogenates were determined as previously described [25, 29]. Lung tissues were homogenized, and the supernatant was collected via centrifugation at 12,000 rpm for 10 min at 4 °C. The supernatant was mixed with substrate solution (0.0005% hydrogen peroxide and 0.167 mg/mL *o*-dianisidine dihydrochloride in pH 6.0 phosphate buffer) and incubated for 15 min. The absorbance of the mixtures at 460 nm was recorded. The protein concentration of the supernatant was determined using a Bio-Rad assay kit. The protein concentration and MPO activity of samples were calculated using a standard curve derived from commercial BSA and MPO, respectively. The results are presented as MPO units/sample protein concentration. Neutrophil elastase activity was determined as described previously [25]. Specifically, supernatants (20 μL) were transferred to 96- well plates, and substrate solution (500 μM, 80 μL) was added immediately. Following incubation at 37 °C for 6 h, the absorbance at 405 nm was recorded. The amount of HNE in tissues was calculated using the calibration curve prepared with HNE and presented as neutrophil elastase (μg)/sample protein concentration (mg).

2.13 H&E and IHC staining

Lung tissues were fixed with 10% formalin overnight and then embedded in paraffin wax. The lung microsections (six microns) were then processed via H&E staining. IHC staining was conducted by an automatic IHC staining device (Vision BioSystems, Australia) using anti-MPO antibody (1:200, dilution) following the manufacturer's protocols. Images were obtained using an Olympus IX81 microscope (Tokyo, Japan).

2.14 Statistical analysis

All results are presented as the mean ± SEM. Differences between control and treatment groups were evaluated using Student's *t*-test or one-way ANOVA as appropriate with GraphPad Prism 5 (San Diego, CA, USA). Statistical significance was indicated by $P < 0.05$.

3. Results

3.1 Isolation and identification of PVAP from P. vulgaris spikes

To isolate new inhibitors of HNE from TCMs, 75 water extracts of TCMs were prepared, and their inhibitory effects on HNE activity were evaluated. Among them, PVW exhibited moderate inhibitory effects against HNE activity with an IC_{50} of 8.08 ± 1.28 μg/mL. Therefore, PVW was chosen as a candidate to identify new anti-HNE agents.

Using a bioactivity-guided fractionation protocol, a crude polysaccharide fraction of PVW was precipitated, and it exerted more potent inhibitory effects on HNE. This fraction was further to fractionated via molecular weight and acetic acid precipitation. The collected precipitate (PVAP) displayed the most potent inhibitory effects against HNE (Table 1).

3.2 Physicochemical properties of PVAP

The carbohydrate, protein, uronic acid, and lignin contents in PVAP were 11.94%, 17.07%, 15.61%, and 19.33%, respectively. The monosaccharide composition of PVAP was analyzed as described previously [26]. The results indicated the PVAP was composed of galactose, glucose, galacturonic acid, arabinose, mannose, rhamnose, and xylose at a ratio of 2.05:1.61:1.59:1.04:1.00:1.00:0.74. To investigate the amino acid residues in degraded PVAP, PVAP was subjected to reductive alkaline degradation and then subjected to amino acid analysis [28]. The results identified 15 amino acid residues. Of these, aspartic acid, glycine, glutamic acid, isoleucine, and cysteine were the major amino acids in PVAP (Table 2).

3.3 PVAP treatment attenuates LPS-induced lung injury in mice

Because PVAP potently and specifically inhibited HNE *in vitro*, PVAP was further examined to determine its effects on an LPS-induced ALI in mice. To determine changes in capillary permeability and the occurrence of lung tissue swelling, the W/D ratio of the lungs was recorded. The results indicated that the lung W/D ratio was significantly increased after LPS exposure, and this value was reversed by PVAP pretreatment (Fig. 1A). The morphological and histological results also confirmed that PVAP pretreatment improved several pathological features, including inflammatory cell infiltration, alveolar cell destruction, and thickening of the alveoli, induced by LPS treatment (Fig. 1B). These results emphasize the protective effects of PVAP against LPS-induced ALI.

3.4 PVAP suppresses HNE and MPO activities and inhibits neutrophil infiltration and NET formation

Neutrophil infiltration and HNE and MPO expression are associated with the progression of ALI [1, 30]. To study the effects of PVAP on ALI, BALF and lung tissues of mice were collected, and the protective effects

of PVAP were determined by analyzing total protein content and MPO and HNE activities. Our data indicated that MPO and HNE activities were significantly augmented in the lung tissue of LPS-treated mice compared with that in control mice. By contrast, pretreatment with PVAP suppressed MPO and HNE activities in a dose-dependent manner (Fig. 2A,B). Indeed, the total protein levels and neutrophil counts in BALF and IHC staining results suggested that PVAP treatment dramatically decreased neutrophil infiltration (Fig. 2C–E).

3.5 PVAP decreases NET formation and cytokine expression in BALF

NETs comprise an extracellular meshwork of decondensed chromatin and antimicrobial proteins that were detected during the progression of ALI, and they promoted LPS-induced synthesis and the release of IL-6 and TNF-α [4, 31]. Furthermore, NET formation was modulated by MPO and HNE [32, 33]. NET formation and IL-6 and TNF-α levels in BALF were measured using commercial kits. The results demonstrated that NET formation and IL-6 and TNF-α expression were meaningfully increased in the BALF of LPS-treated mice compared with the findings in control mice, whereas these findings were ameliorated by PVAP pretreatment (Fig. 3A–C).

4. Discussion

Polysaccharides, which are macromolecules composed of long chains of monosaccharide units, are the key bioactive components of TCMs, and they possess immunomodulatory, antitumor, anti-inflammatory, hypoglycemic, anti-aging, and antioxidant effects [34–37]. In our previous study, the polysaccharide KSWP was isolated from *Kochia scoparia* fruit. KSWP exhibited selective inhibitory effects against HNE with an IC_{50} of 3.74 ± 0.46 μg/mL, thereby attenuating LPS-mediated ALI [25]. The present study results suggest that PVAP is slightly more potent than KSWP, and it also appears to have stronger protective effects *in vivo*. Therefore, TCMs could serve as sources for isolating HNE inhibitors.

Many polysaccharides or polysaccharide-containing fractions have been isolated from *P. vulgaris*. Among them, three water-soluble polysaccharides (PV-P1–P3) and a polysaccharide (P1) that enhanced NO, TNF-α, and IL-6 production in RAW264.7 cells were isolated by Li and co-workers [38, 39]. Subsequently, a zinc-conjugating derivative of P1 (P1-Zn) was synthesized. P1-Zn significantly inhibited the proliferation of a human hepatocellular carcinoma cell line (HepG2) by inducing apoptosis [40]. Two polysaccharides, namely PW-S1 and PW-S2, inhibited anti-complement activity through suppressing the classical and alternative pathways [23]. Another polysaccharide (P32) exhibited anti-lung adenocarcinoma activity via immunostimulatory effects [24]. Additionally, polysaccharides or polysaccharide-containing fractions of *P. vulgaris* (PSP-2B, PPV, and PPS-2b) displayed inhibitory effects against herpes virus *in vitro* and *in vivo* [41–43]. In the present study, a polysaccharide-containing fraction (PVAP) was obtained using a bioactivity-guided fractionation protocol. This is the first

polysaccharide from *P. vulgaris* that prevented ALI through the selective inhibition of HNE. Therefore, it could represent a candidate for manipulating HNE level homeostasis and preventing ALI.

Xylose and arabinose are the major monosaccharides in most polysaccharides of *P. vulgaris* excluding PPS-2b and PW-S2 [23, 38–43]. PVAP had a slightly different monosaccharide composition as PPS-2b, which was composed of glucose, galactose, mannose, galacturonic acid, xylose, rhamnose, and arabinose at a molar ratio of 3.1:1.0:0.7:0.5:0.3:0.3:0.1. In addition, PVAP also contained 19.33% lignin according to the acetyl bromide method, and its absorption maxima were recorded at approximately 210 and 280 nm, suggesting that PVAP is also a lignin–carbohydrate complex [43].

5. Conclusion

PVAP was obtained as a bioactive fraction from the PVW using a bioactivity-guided fractionation protocol. Our data demonstrated that PVAP could prevent LPS-induced ALI *in vivo* through selectively inhibiting HNE activity. Accordingly, PVAP can be a candidate for developing HNE inhibitors.

Abbreviations

ALI
Acute lung injury
ARDS
Acute respiratory distress syndrome;
BALF
Bronchoalveolar lavage fluid
BSA
bovine serum albumin
CG
Cathepsin G
ELISA
Enzyme-linked immunosorbent assay
HNE
Human neutrophil elastase
H&E
Haematoxylin and eosin
IHC
Immunohistochemistry
PVAP
Fraction from the water extracts of *Prunella vugaris*
LPS
Lipopolysaccharide
MPO

Myeloperoxidase
NETs
Neutrophil extracellular traps
PR3
Proteinase 3
PMP
1-Phenyl-3-methyl-5-pyrazolone;
TCMs
Traditional Chinese medicines.

Declarations

Availability of data and materials

All datasets used in this study are available through the corresponding author on reasonable application.

Ethics approval and consent to participate

All animal research procedures were reviewed and approved by the Institutional Animal Care and Use Committee of Chang Gung University (Taoyuan, Taiwan, IDs CGU105-019 and CGU16-079).

Consent for publication

Not applicable.

Competing interests

All authors declare that they have no competing interests.

Author contributions

Conception and design of the research: H.P.Y., and P.W.H.; performed experiments: C.L.C.; acquired and analyzed data: C.L.C., H.P.Y., and P.W.H.; drafted and edited the manuscript: C.L.C., and P.W.H.; assisted with experiments: K.Y.C, Y.L.C. and K.J.C, Y.L.H.; data discussion and review of the manuscript; C.L.C., H.P.Y., and P.W.H.. Huang-Ping Yu and Chieh-Lun Cheng contributed equally to this work.

Acknowledgements

We thank the technique supports from Bioproduction Engineering Technology Department, Biomedical Technology and Device Research Laboratories, ITR (Hsinchu, Taiwan) for performing genomic analysis and amino acids analysis of plant material.

Funding

This work was supported by the Ministry of Science and Technology grants (MOST106-2320-B-182-003-MY3) and the Chang Gung Memorial Hospital grants (CMRPD1F0561-2, CMRPD1I0021-2 and BMRPB23) to P.-W. Hsieh. The funders had no role in the study design, the data collection and analysis, the decision to publish, or the preparation of the manuscript.

References

1. Gao F, Liu X, Shen Z, Jia X, He H, Gao J, Wu J, Jiang C, Zhou H, Wang Y. Andrographolide sulfonate attenuates acute lung injury by reducing expression of myeloperoxidase and neutrophil-derived proteases in mice. Front Physiol. 2018;9:939.
2. Gill SF, Yamashita CM, Veldhuizen RAW. Lung remodeling associated with recovery from acute lung injury. Cell Tissue Res. 2017;367:495–509.
3. Polverino E, Mayor ER, Dale GE, Dembowsky K, Torres A. The role of neutrophil elastase inhibitors in lung diseases. Chest. 2017;152:249–62.
4. Lee JM, Yeo CD, Lee HY, Rhee CK, Kim IK, Lee DG, Lee SH, Kim WJ. Inhibition of neutrophil elastase contributes to attenuation of lipopolysaccharide-induced acute lung injury during neutropenia recovery in mice. J Anesth. 2017;31:397–404.
5. Li H, Zhou X, Tan H, Hu Y, Zhang L, Liu S, Dai M, Li Y, Li Q, Mao Z, Pan P, Su X, Hu C. Neutrophil extracellular traps contribute to the pathogenesis of acid-aspiration-induced ALI/ARDS. Oncotarget. 2018;9:1772–84.
6. Tsai YF, Hwang TL. Neutrophil elastase inhibitors: a patent revies and potential applications for inflammatory lung diseases (2010–2014). Expert Opin Ther Pantents. 2015;25:1145–58.
7. Chen YL, Hwang TL, Yu HP, Fang JY, Chong KY, Chang YW, Chen CY, Yang HW, Chang WY, Hsieh PW. *Ilex kaushue* and its bioactive component 3,5-dicaffeoylquinic acid protected mice from lipopolysaccharide-induced acute lung injury. Sci Rep. 2016;6:34243.
8. Ishii T, Doi K, Okamoto K, Imamura M, Dohi M, Yamamoto K, Fujita T, Noiri E. Neutrophil elastase contributes to acute lung injury induced by bailateral nephrectomy. Am J Pathol. 2010;177:1665–73.
9. Kim E, Choi A, Nam H. Drug repositioning of herbal compounds via a machine-learning approach. BMC Bioinformatics. 2019;20:247.

10. Pan SY, Chen SB, Dong HG, Yu ZL, Dong JG, Long ZX, Fong WF, Han YF, Ko KM. New perspectives on Chinese herbal medicine (Zhong-Yao) research and development. Evid Based Complement Alternat Med. 2011;2011:403709.
11. Pan SY, Zhou SF, Gao SH, Yu ZL, Zhang SF, Tang MK, Sun JN, Ma DL, Han YF, Fong WF, Ko KM. New Perspectives on How to Discover Drugs from Herbal Medicines: CAM's Outstanding Contribution to Modern Therapeutics. Evid Based Complement Alternat Med 2013; 2013:627375.
12. Wang H, Si S, Wang S. Can hightly cited herbs in ancient traditional Chinese medicine formulas and modern publications predict therapeutic targets for diabetes mellitus? J Ethnopharmacol. 2018;213:101–10.
13. Bai Y, Xia B, Xie W, Zhou Y, Xie J, Li H, Liao D, Lin L, Li C. Phytochemistry and pharmacological activities of the genus *Prunella*. Food Chem. 2016;204:483–96.
14. Caleja C, Finimundy TC, Pereira C, Barros L, Calhelha RC, Sokovic M, Lvanov M, Carvalho AM, Rosa E, Ferreira ICFR. Challenges of traditional herbal teas: plant infusions and their mixtures with bioactive properties. Food Funct. 2019;10:5939–51.
15. Chen Y, Zhang X, Guo Q, Cao L, Qin Q, Li C, Zhao M, Wang W. Plant morphology, physiological characteristics, accumulation of secondary metabolites and antioxidant activities of *Prunella vulgaris* L. under UV solar exclusion. Biol Res. 2019;52:17.
16. Kim J, Cho K, Choung SY. Protective effect of *Prunella vulgaris* var. L extract against blur light induced damages in ARPE-19 cells and mouse retina. Free Radic. Biol. Med. 2020; in press.
17. Komal S, Kazmi SAJ, Khan JA, Gilani MM. Antimicrobial activity of *Prunell vulgaris* extracts against multi-drug resistant *Escherichia coli* from patients of urinary tract infection. Pak J Med Sci. 2018;34:616–20.
18. Li BY, Hu Y, Li J, Shi K, Shen YF, Zhu B, Wang GX. Ursolic acid from *Prunella vulgaris* L. efficiently inhibits IHNV infection in vitro and in vivo. Virus Res. 2019;273:197741.
19. Kajima H, Tominga H, Sato S, Ogura H. Pentacyclic triterpenoids from *Prunella vulgaris*. Phytochemistry. 1987;26:1107–11.
20. Ryu SY, Lee CK, Lee CO, Kim HS, Zee OP. Antiviral triterpenes from *Prunella vulgaris*. Arch Pharm Res. 1992;15:242–5.
21. Li HM, Kim JK, Jang JM, Kwon SO, Cui CB, Lim SS. The inhibitory effect of *Prunella vulgaris* L. on aldose reductase and protein glycation. J Biomed Biotechnol. 2012;10:928159.
22. Wang ZJ, Zhao YY, Wang B. Depsides from *Prunella vulgaris*. Chinese Chem Lett. 2000;11:997–110.
23. Du D, Lu Y, Cheng Z, Chen D. Structure characterization of two novel polysaccharides isolated from the spikes of *Prunella vulgaris* and their anticomplement activities. J Ethnopharmacol. 2016;193:345–53.
24. Feng L, Jia XB, Shi F, Chen Y. Identification of two polysaccharides from *Prunella vulgaris* L. and evaluation on their anti-lung adenocarcinoma activity. Molecules. 2010;15:5093–103.

25. Chen YL, Hwang TL, Fang JY, Lan YH, Chong KY, Hsieh PW. Polysaccharides from *Kochia scoparia* fruits protect mice from lipopolysaccharide-mediated acute lung injury by inhibiting neutrophil elastase. J Funct Foods. 2017;38:582–90.
26. Tseng CP, Huang YL, Chang YW, Liao HR, Chen YL, Hsieh PW. Polysaccharide-containing fraction from *Artemisia argyi* inhibits tumor cell-induced platelet aggregation by blocking interaction of podoplanin with C-type lectin-like receptor 2. J Food Drug Anal. 2020;28:115–23.
27. Moreira-Vilar FC, Siqueira-Soares RdeC, Finger-Teixeira A, de Oliverira DM, Ferro AP, da Rocha GJ, Ferrarese MdeL, dos Santos WD, Ferrarese-Filho O. The acetyl bromide method is faster, simpler and presents best recovery of lignin in different herbaceous tissues than Klason and thioglycolic acid methods. PLoS One. 2014;16:e110000.
28. Qin X, Yamauchi R, Aizawa K, Inakuma T, Kato K. Structural features of arabionogalactan-proteins from the fruit of *Lycium chinense* Mill. Carbohydr Res. 2001;333:79–85.
29. Chang YW, Tseng CP, Lee CH, Hwang TL, Chen YL, Su MT, Chong KY, Lan YW, Wu CC, Chen KJ, Lu FH, Liao HR, Hsueh C, Hsieh PW. β-Nitrostyrene derivatives attenuate LPS-mediated acute lung injury via the inhibition of neutrophil-platelet interactions and NET release. Am J Physiol Lung Cell Mol Physiol. 2018;314:L654–69.
30. Okeke EB, Louttit C, Fry C, Najagabadi AH, Han K, Nemzek J, Moon JJ. Inhibition of neutrophil elastase prevents neutrophil extracellular trap formation and rescues mice from endotoxic shock. Biomaterials. 2020;238:119836.
31. Zou Y, Chen X, Xiao J, Zhou DB, Lu XX, Li W, Xie B, Kuang X, Chen Q. Neutrophil extracellular traps promote lipopolysaccharide-induced airway inflammation and mucus hypersecretion in mice. Oncotarget. 2018;9:13276–86.
32. Majewski P, Majchrzak-Gorecka M, Grygier B, Skrzeczynska-Moncznik J, Osiecka O, Cichy J. Inhibitors of serine proteases in regulating the production and function of neutrophil extracellular traps. Front Immunol. 2016;7:261.
33. Papayannopoulos V, Metzler KD, Hakkim A, Zychlinsky A. Neutroophil elastase and myeloperoxidase regulate the formation of neutrophil extracellular traps. J Cell Biol. 2010;191:677–91.
34. Chen Y, Yao F, Ming K, Wang D, Hu Y, Liu J. Polysaccharides from traditional Chinese medicines: extraction, purification, modification, and biological activity. Molecules. 2016;21:1705.
35. Kikete S, Luo L, Jia B, Wang L, Ondieki G, Bian Y. Plant-derived polysaccharides active dendritic cell-based anti-cancer immunity. Cytotechnology. 2018;70:1097–110.
36. Liu Y, Huang G. Extraction and derivatisation of active polysaccharides. J Enz Inh Med Chem. 2019;34:1690–6.
37. Zheng Y, Bai L, Zhou Y, Tong R, Zeng M, Li X, Shi J. Polysaccharides from Chinese herbal medicine for anti-diabetes recent advances. Int J Biol Marcomol. 2019;121:1240–51.
38. Li C, Huang Q, Fu X, Yue XJ, Liu RH, You LJ. Characterization, antioxidant and immunomodulatory activities of polysaccharides from *Prunella vulgaris* Linn. Int J Biol Marcomol. 2015;75:298–305.

39. Li C, You L, Fu X, Huang Q, Yu S, Liu RH. Structural characterization and immunomodulatory activity of a new heteropolysaccharide from *Prunella vulgaris*. Food Funct. 2015;6:1557–67.
40. Li C, Huang Q, Xiao J, Fu X, You L, Liu RH. Preparation of *Prunella vulgaris* polysaccharide-zinc complex and its antiproliferative activity in HepG2 cells. Int J Biol Marcomol. 2016;91:671–9.
41. Chiu LCM, Zhu W, Ooi VEC. A polysaccharide fraction from medicinal herb *Prunella vulgaris* downregulates the expression of herpes simplex virus antigen in Vero cells. J Ethnopharmacol. 2004;93:63–8.
42. Ma FW, Kong SY, Tan HS, Wu R, Xia B, Zhou Y, Xu HX. Structural characterization and antiviral effect of a novel polysaccharide PSP-2B from Prunellae spica. Carbohydr Polym. 2016;152:699–709.
43. Zhang Y, But PPH, Ooi VEC, Xu HX, Delaney GD, Lee SHS, Lee SF. Chemical properties, mode of action, and in vivo anti-herpes activities of a lignin-carbohydrate complex from *Prunella vulgaris*. Antiviral Res. 2007;75:242–9.

Tables

Table 1. Neutrophil serine proteases inhibition profiles of PVW and PVAP.

	IC_{50} (mg/mL)[a]		
	HNE[b]	CG[b]	PR3[b]
PVW	8.08 ± 1.28	> 300	138.18 ± 7.99
PVAP	2.42 ± 0.19	> 300	> 300
Sivelastat[c]	0.019 ± 0.001	□	0.229 ± 0.037
CG inhibitor[c]	□	0.097 ± 0.0018	□

[a]Data was presented as mean ± S.E.M. (n ≥ 3).

[b]HNE: human neutrophil elastase. PR3: protienase 3. CG: cathepsin G.

[c]Sivelastat and CG inhibitor were used as positive controls.

Table 2. Amino acid analysis of reductive alkaline degraded PVAP.

Amino acids	W/W%	Amino acids	W/W%
L-Asp	12.10	L-Ile	8.75
L-Thr	3.92	L-Leu	1.86
L-Ser	4.25	L-Tyr	3.65
L-Glu	15.92	L-Phe	6.05
Gly	14.21	L-Lys	3.44
L-Ala	7.04	L-His	1.27
L-Cys	8.40	L-Arg	4.23
L-Val	4.91		

Figures

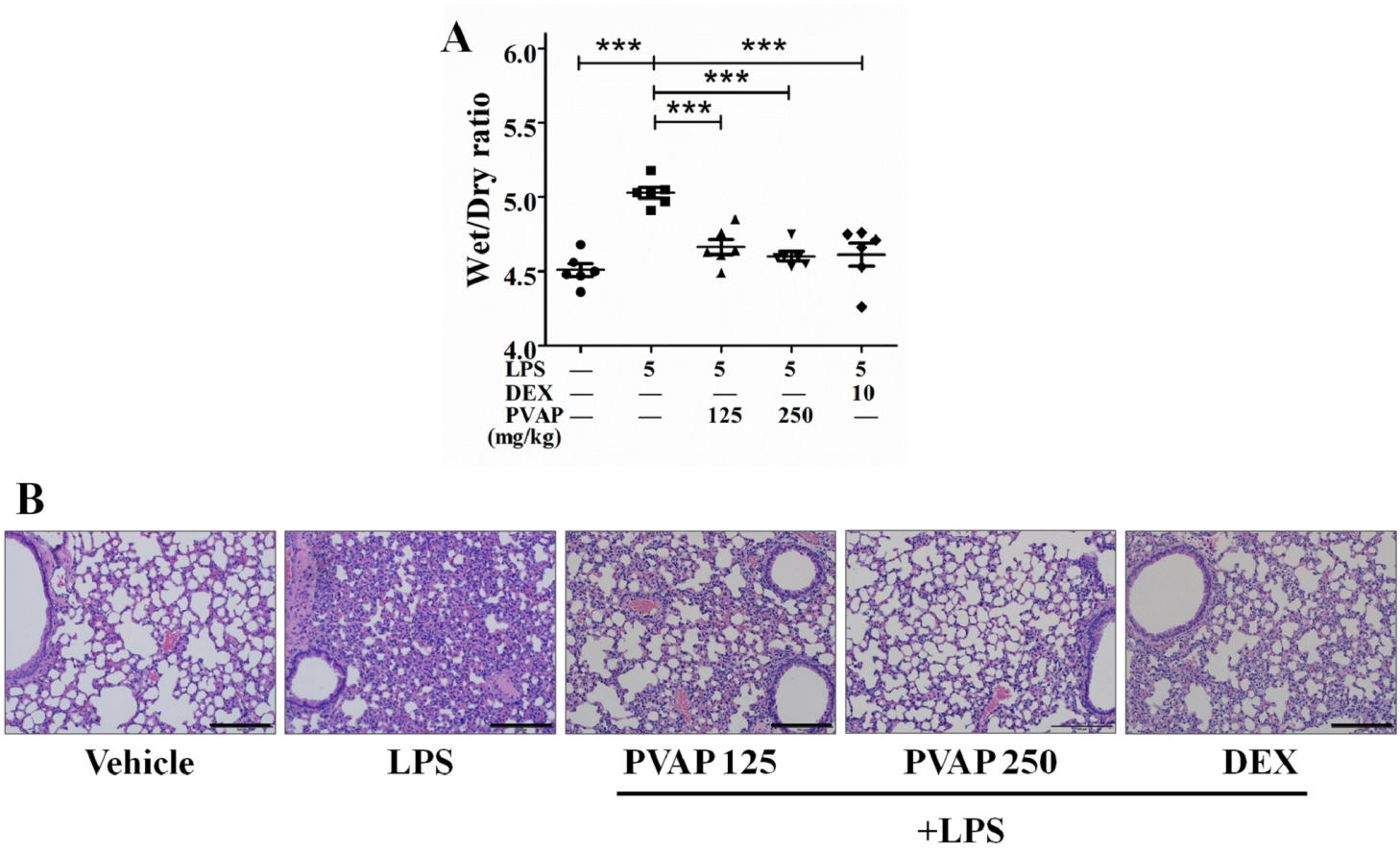

Figure 1

The bioactive fraction of the water extract of Prunella vulgaris spikes (PVAP) reduced lung edema and pathological changes in mice with lipopolysaccharide (LPS)-induced acute lung injury. Mice were pretreated with vehicle, PVAP (125 and 250 mg/kg), or dexamethasone (DEX, 10 mg/kg) before exposure to LPS (5 mg/kg) through intratracheal instillation for 6 h. (A) The lung wet/dry weight ratio was determined to evaluate pulmonary edema after LPS treatment. (B) A photomicrograph of hematoxylin and eosin-stained lung sections was obtained via light microscopy. Scale bar = 100 μm. Data are shown as the mean ± SEM of six independent experiments. ***P < 0.001 compared with the LPS-treated group.

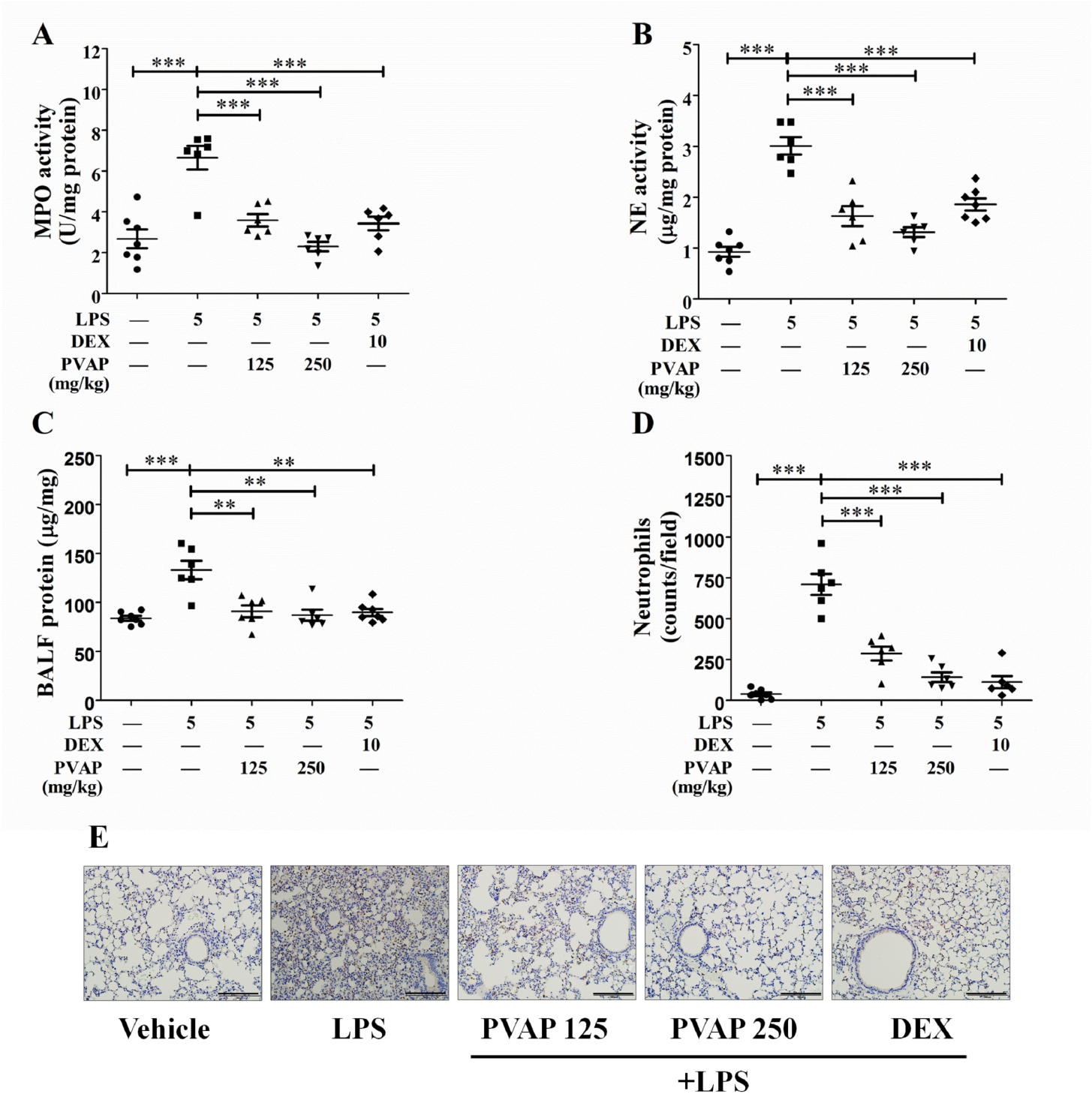

Figure 2

The bioactive fraction of the water extract of Prunella vulgaris spikes (PVAP) attenuated myeloperoxidase (MPO) and human neutrophil elastase (HNE) activities and inhibited neutrophil infiltration in mice with lipopolysaccharide (LPS)-induced acute lung injury (ALI). PVAP pretreatment protected against ALI induced by LPS in mice. ICR mice were treated with vehicle, PVAP (125 and 250 mg/kg), or dexamethasone (DEX, 10 mg/kg) through gavage before LPS treatment. Bronchoalveolar lavage fluid

(BALF) and tissue samples were collected after 6 h of LPS treatment. (A) MPO and (B) HNE levels in lung tissues. (C) Total protein concentration and (D) the number of neutrophils in BALF. (E) Immunohistochemical staining of MPO (brown) in lung sections. Scale bar = 100 μm. Data are shown as the mean ± SEM of six independent experiments. **P < 0.005 and ***P < 0.001 compared with the LPS-treated group

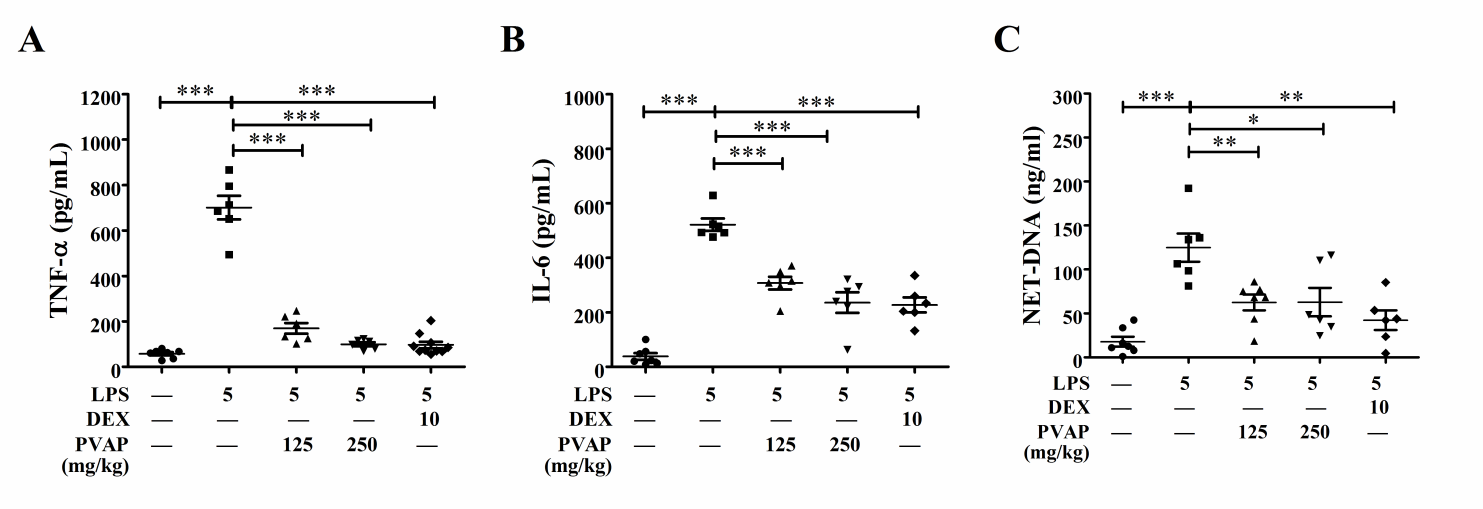

Figure 3

The bioactive fraction of the water extract of Prunella vulgaris spikes (PVAP) reduced the levels of pro-inflammatory cytokines and neutrophil extracellular trap (NET) formation. Pro-inflammatory cytokine (TNF-α and IL-6) and NET DNA levels were examined in the supernatant of centrifuged bronchoalveolar lavage fluid. (A) TNF-α; (B) IL-6; (C) NET DNA. Data are shown as the mean ± SEM of six independent experiments. **P < 0.005 and ***P < 0.001 compared with the LPS-treated group.

Supplementary Files

This is a list of supplementary files associated with this preprint. Click to download.

- Supportinginformation.docx
- Supportinginformation.docx